

Synthesis, Characterization, and Evaluation of Metal–Organic Frameworks for Oxidative Desulfurization: An Integrated Experiment

Ernesto Lucatero, Robabeh Bashiri, and Monica C. So*



Cite This: *J. Chem. Educ.* 2024, 101, 3428–3433



Read Online

ACCESS |

Metrics & More

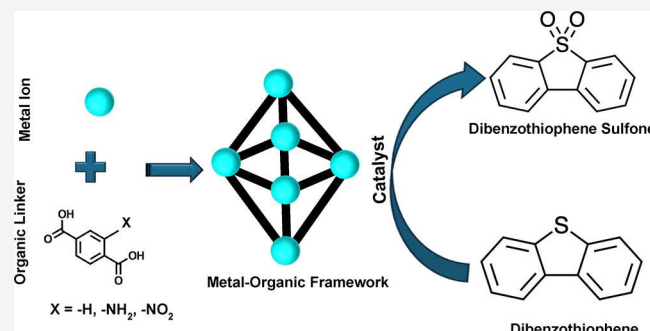
Article Recommendations

Supporting Information

ABSTRACT: Herein, we present an integrated upper division chemistry laboratory experiment involving the synthesis, characterization, and evaluation of catalytic metal–organic frameworks (MOFs). Experiments are designed to facilitate the solvothermal synthesis and characterize MOFs, including UiO-66, UiO-66-NH₂, and UiO-66-NO₂. The MOFs are employed as catalysts in oxidative desulfurization (ODS) of an organic sulfur-containing compound, dibenzothiophene (DBT), in a laboratory experiment. To investigate the composition and structure of the MOFs, powder X-ray diffraction (PXRD) and elemental analysis (EA), respectively, are employed. Using Fourier transform infrared (FT-IR) spectroscopy, students evaluate the different organic linkers found

in the MOFs. Students then investigate the effects of the electronic environment of the organic linker of the MOFs on the ODS of DBT. Students find that all three porous and crystalline MOFs oxidize DBT, but UiO-66-NO₂ exhibits the most efficient catalytic conversion.

KEYWORDS: *Upper-Division Undergraduate Laboratory, Hands-on Learning/Manipulatives, Collaborative/Cooperative Learning, Physical Properties, Undergraduate Research, Laboratory Instruction, Metal–Organic Frameworks, UiO-66, UiO-66-NH₂, UiO-66-NO₂, Dibenzothiophene, Oxidative Desulfurization*



INTRODUCTION

Endowed with both high surface area and chemical and synthetic modularity, metal–organic frameworks (MOFs) are hybrid organic–inorganic materials which can be used for a plethora of applications, such as water decontamination,¹ energy conversion,^{2–4} gas capture/storage,^{5,6} and catalysis.^{7–10} Catalytic activity may originate from the tunability of the organic linkers^{11,12} and metal sites.^{13–16} The versatility and strategic positioning of these catalytic sites are what make MOFs an ideal choice for heterogeneous catalysis.¹⁷

Since MOFs are synthesized through facile methods and their structures and chemistry are easily tunable, these aspects allow undergraduate laboratories to incorporate MOF-based experiments into their curriculum.^{3,18} Using MOFs for catalysis as a learning tool in laboratories introduces undergraduate students to reaction kinetics, electron withdrawing/donating functional groups, and solid-state materials chemistry, serving as a crossroads between general, organic, and inorganic chemistry. This approach underscores the importance of research-based learning in chemistry, bridging the gap between textbook knowledge and real-world scientific research. Engaging with MOFs in an educational setting enables students to experience firsthand the application of cutting-edge materials science, thereby fostering a more comprehen-

sive and hands-on educational experience in the field of chemistry.

While earlier studies have made significant efforts to understand catalytic processes in a research setting,^{19–24} undergraduate students' exposure to oxidative desulfurization (ODS) remains notably limited in the teaching laboratories, despite the critical role of ODS in desulfurization of fuels. This gap underscores the need for further attention and exploration in this subject area. Previously, Jannsens *et al.* performed esterification reactions with a polyoxometalate (POM), a class of nanoclusters, as a catalyst for the reaction. When the catalytic POM is encapsulated by the copper-based MOF, HKUST-1, the POM can be recovered, emphasizing the recyclability of the catalyst.²⁵ Huo *et al.* on the other hand, used NENU-9, another copper-based MOF,²⁶ to demonstrate ODS of dibenzothiophene (DBT) which introduced students

Received: March 13, 2024

Revised: July 9, 2024

Accepted: July 12, 2024

Published: July 23, 2024



to heterogeneous catalysis and to train students on aiming to solve environmental issues with their skill sets.

This work, however, differs from previous work in three ways. First, this is the first upper-division laboratory experiment where students investigate the effects of the electronic effects of the organic linkers on catalytic efficiency in the ODS reaction of DBT. The MOFs vary by the addition of an electron-donating group (UiO-66-NH_2), or an electron-withdrawing group (UiO-66-NO_2), or the lack thereof (UiO-66) within their organic linker. Second, this experiment focuses on utilizing the zirconium-based Lewis acid metal sites in the UiO-66 series of MOFs for catalysis, unlike the copper-based sites in previous works. Due to the multiple zirconium-oxo bonds that strongly bind the zirconium-based MOFs together, these MOFs result in higher chemical and thermal stability. Lastly, this laboratory experiment emphasizes the application of interdisciplinary chemistry concepts, which span from general to organic, inorganic, and materials chemistry. Thus, in this laboratory experiment, we demonstrate how the electron-withdrawing effects of the organic linker in three zirconium-based MOFs affect the overall catalytic conversion of DBT to its oxidized form, DBTO_2 . This experiment ultimately offers undergraduates a greater understanding of interdisciplinary concepts within the field of inorganic materials chemistry.

EXPERIMENTAL SECTION

This procedure is designed for upper-division chemistry and biochemistry majors to apply their skills from previous courses, such as general chemistry, organic chemistry, analytical chemistry, and inorganic chemistry, in a single integrated lab experience. This section is divided into three steps, including synthesis, characterization, and catalytic performance evaluation of each MOF.

As described in Figure 1, UiO-66 and UiO-66-NH_2 were synthesized. Both involved sonicating zirconium(IV) tetrachloride (ZnCl_4) and 1 mL of 6 M HCl in 5 mL of dimethylformamide (DMF) for 20 min. This was then followed by sonication of the organic linkers, terephthalic acid for UiO-66 and 2-aminoterephthalic acid for UiO-66-NH_2 , in 10 mL of DMF for 20 min. The solution was then

placed within an oven at 80 °C for 24 h in order to initiate the solvothermal reaction. Then the formed precipitate was centrifuged and underwent solvent exchange from DMF to ethanol (EtOH). The washed precipitate was last activated at 90 °C for 24 h.

UiO-66-NO_2 was synthesized similarly. Zirconium(IV) tetrachloride and 2-nitrotetraphthalic acid were dissolved and sonicated in 10 mL of DMF for 20 min, followed by the addition of 32.5 μL of deionized (DI) water and sonicated for another 20 min. A Teflon lined stainless-steel autoclave was used to heat the solution to 120 °C for 24 h. The formed precipitate was centrifuged and underwent a solvent exchange from DMF to EtOH. The washed precipitate was last activated at 90 °C for 24 h.

The MOFs were then characterized by Fourier transform infrared spectroscopy (FT-IR) to confirm the presence of functional groups of the organic linker, powder X-ray diffraction (PXRD) to determine the crystallinity of the material, and elemental analysis (EA) to confirm the elemental composition. Nitrogen isotherms were collected to evaluate the surface areas and pore diameters of the MOFs.

To examine the catalytic performance of the MOFs, an ODS is performed. A model oil was first prepared with dibenzothiophene in acetone and a known sample of benzophenone as our internal standard. In the 3-neck round-bottom flask, the MOF was introduced to 30% H_2O_2 followed by the model oil. The round-bottom flask would then be connected to a reflux reaction system and heated through an oil bath. The reaction was monitored to keep an internal temperature of 60 °C.

GC-MS samples were taken throughout the reaction from 0 to 2 h and ran under a known ODS of DBT in acetone method. The concentration of oxidized dibenzothiophene was determined with the known concentration of the IS and the initial response factor determined using eq 1 where A_x is the area of the analyte signal, $[X]_f$ is the concentration of the analyte, A_s is the area of the standard single, $[S]_f$ is the concentration of the standard signal, and F is the response factor.

$$\frac{A_x}{[X]_f} = F \frac{A_s}{[S]_f} \quad (1)$$

SAFETY HAZARDS

To safely conduct the laboratory activity, students should wear lab coats, safety goggles, and gloves. Zirconium(IV) chloride, terephthalic acid, 2-aminoterephthalic acid, 2-nitrotetraphthalic acid, dibenzothiophene, 6 M hydrochloric acid, and 30% hydrogen peroxide may result in eye and skin injuries. If accidentally exposed, eyes and skin should be rinsed with water for a minimum of 15 min. Individuals are advised to seek medical attention immediately afterward. All instructors and students must review the MSDS of the chemicals used in the activity. To ensure that the heat from the hot plate heats the oil bath to 60 °C, the hot plates were set to 130 °C. To avoid accidents, students must wear oven mitts when moving the oil bath.

LEARNING OBJECTIVES AND CONCEPTS

Students gain experience working with MOFs through lecture video and hands-on lab skills acquisition in synthesis and characterization. Before each topic, students watch a lecture

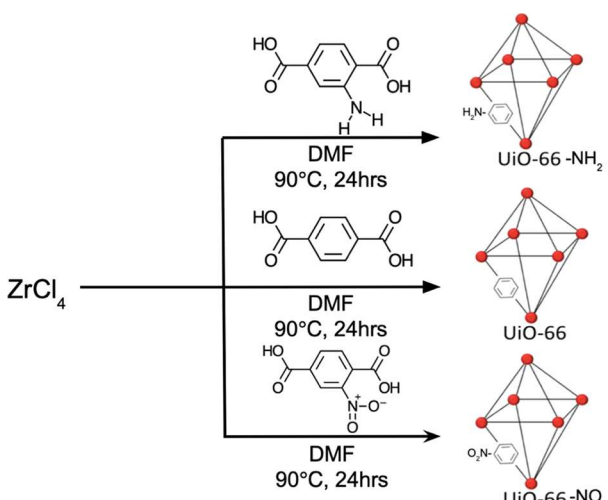


Figure 1. Schematic diagram of solvothermal and hydrothermal synthesis of UiO-66 , UiO-66-NH_2 , and UiO-66-NO_2 .

video to provide the fundamental concepts of each synthesis and characterization procedure. This instruction and hands-on lab work teach students MOF analysis via PXRD, EA, isotherms, FT-IR, and GC-MS. Students track the structural retention of MOFs via the presence of peaks correlated with lattice spacings via PXRD. Using EA and FT-IR, students monitor the elemental and organic composition, respectively, of the MOFs. Finally, GC-MS quantifies the conversion of DBT to DBTO₂ to calculate the catalytic efficiency.

RESULTS AND DISCUSSION

Structural Characterization

The crystallinity, structure, and identity of UiO-66 and its analogues are verified through powder X-ray diffraction (PXRD, Figure 2). Usage of this technique allows students

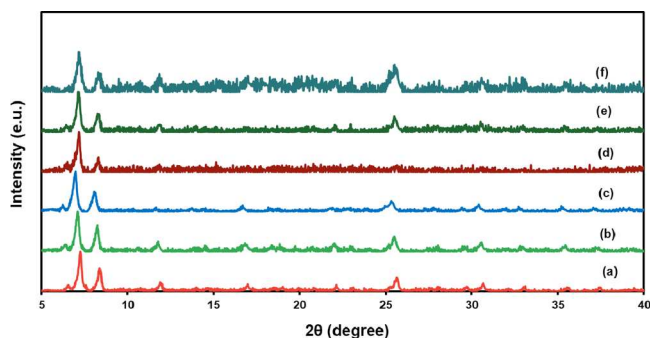


Figure 2. PXRD patterns of as-synthesized (a) UiO-66, (b) UiO-66-NH₂, and (c) UiO-66-NO₂ and post-ODS reaction (d) ODS-UiO-66, (e) ODS-UiO-66-NH₂, and (c) ODS-UiO-66-NO₂.

to explore how X-rays interact with crystalline structures and how a measurement can be made from the interaction. Peaks shown are characteristic of the corresponding UiO-66 family of MOFs. Post-ODS MOFs show that the crystallinity of the UiO-66 powders retained major peaks, but some peaks disappeared or shifted, suggesting introduction of defects into the MOFs; students understood that this indicates that MOF structures slightly change after the reactions (Figure 3).

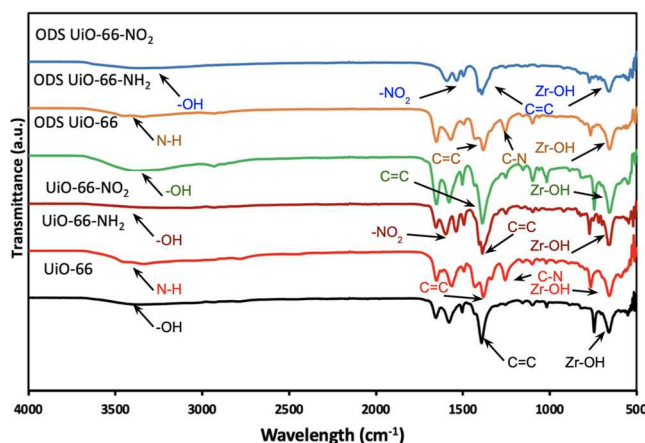


Figure 3. FT-IR of as-synthesized (a) UiO-66, (b) UiO-66-NH₂, and (c) UiO-66-NO₂ and post-ODS reaction (d) ODS-UiO-66, (e) ODS-UiO-66-NH₂, and (c) ODS-UiO-66-NO₂.

Nitrogen Isotherm Analysis

The N₂ isotherms (Figure S2) present type I adsorption isotherms, confirming that UiO-66 and analogues are micro-porous. The surface area of UiO-66 was found to be 854 m²·g⁻¹.²⁷ Noticeably, this value decreases to 485 m²·g⁻¹ and 424 m²·g⁻¹ for UiO-66-NH₂ and UiO-66-NO₂, respectively, after functionalized with -NO₂ and -NH₂. These data are consistent with previously reported work.²⁸ Students learned that after the ODS reaction the surface areas of all catalysts increased (Figure S2b), confirming crystal structure changes and the creation of defects on the surface of the catalysts. However, these changes do not affect the catalytic performance, highlighting the importance of the functionalization of UIO-66 on its catalytic performance.

Elemental Composition

Elemental analysis (EA) data verifies the elemental composition of UiO-66 and its variants. All variants have C, H, O, and Zr, as expected. However, unlike the EA results for UiO-66, the results for UiO-66-NH₂ and UiO-66-NO₂ both confirm the presence of nitrogen, which originates from the amino group on 2-aminoterephthalic acid and nitro group on the 2-nitrotetraphthalic acid. We noted decreases in elements in Table 1 due to structural degradation after the ODS reaction.

Table 1. Elemental Analysis of As-Synthesized and Post-ODS Reactions of Different MOFs

Element	As-synthesized MOFs (mass %)			Post-ODS Reaction MOFs (mass %)		
	UiO-66	UiO-66-NH ₂	UiO-66-NO ₂	UiO-66	UiO-66-NH ₂	UiO-66-NO ₂
C	30.43	29.06	30.00	29.83	28.38	27.75
H	3.11	4.63	4.16	2.72	4.82	2.28
O	47.07	40.57	40.45	42.07	40.13	43.67
N	0	8.05	4.24	0.97	4.82	4.39
Zr	19.39	17.69	21.15	24.41	21.85	21.91

This is consistent with the PXRD data in Figure 2, which shows that some of the peaks in the post-ODS MOFs disappeared or shifted as well as the increase in surface areas of the MOFs in Figure S2b. From this data, the students learn that the ODS reaction introduces defects into the MOFs.

Organic Linker Identity

FT-IR spectroscopy was used to determine the structure of the organic linker within the UiO-66 variants, as well as the different functional groups within each MOF. All assignments are summarized in Table 2. UiO-66 showed a wide broad peak

Table 2. FT-IR Assignments of the As-Synthesized MOFs

MOF	Functional group	Wavenumber (cm ⁻¹)
UiO-66	-OH	3305
	C=C	1500
	Zr-OH	600–700
	-OH	3300
	-NO ₂	1550
	C=C	1480
UiO-66-NO ₂	Zr-OH	600–700
	N-H	3400
	C-N	1350
	C=C	1500–1700
	Zr-OH	600–700
UiO-66-NH ₂		

that appeared at around 3305 cm^{-1} which indicates the formation of O–H bonds from hydrogen bonds within the zirconium–oxygen cluster in the organic linker. The bending at around 1500 cm^{-1} suggests the presence of a C=C bond that forms from the carbonyl present in the zirconium–oxygen cluster. The Zr–O cluster bending can also be found in the peaks located in the range 600 – 700 cm^{-1} . UiO-66-NH_2 showed a wide broad peak at 3400 cm^{-1} indicating the presence of a N–H bond from the amine. Another amine functional group peak is present at 1350 cm^{-1} indicative of C–N bond stretching. The C=C peak from the carbonyl present in the Zr–O cluster can be seen in the 1500 – 1700 cm^{-1} range. UiO-66-NH_2 also contains the peaks indicative of the Zr–O cluster from 600 to 700 cm^{-1} . UiO-66-NO_2 showed a strong $-\text{NO}_2$ peak at 1550 cm^{-1} . The stretching from the C=C bond is seen at 1480 cm^{-1} and the stretching from the Zr–O cluster can be found at 550 cm^{-1} (Figure 3). FT-IR data were collected for as-synthesized and post-ODS reactions, but only IR assignments for as-synthesized reactions are included in Table 1 because they did not change after the reaction. Therefore, the students understood that the functional group vibrations are retained after the ODS reaction (Figure 3).

Catalytic Performance Measurements

Oxidative desulfurization of DBT in acetone was monitored by GC-MS at various time points (0, 0.5, 1.5, and 2 h) as shown in GC-MS plots in Figures S3 and S4 as well as Figure 4. UiO-66

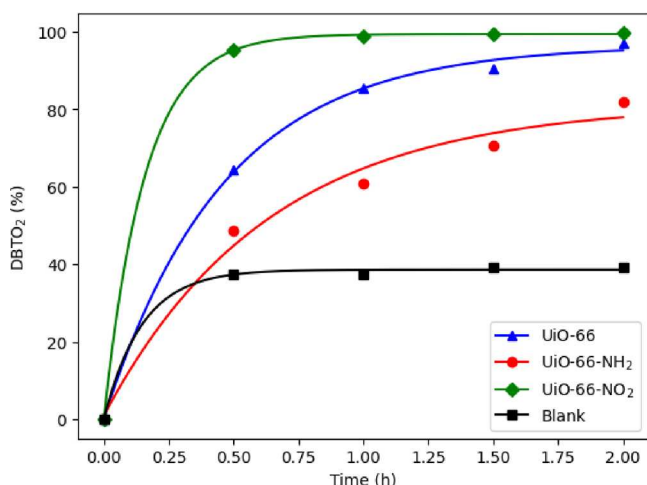


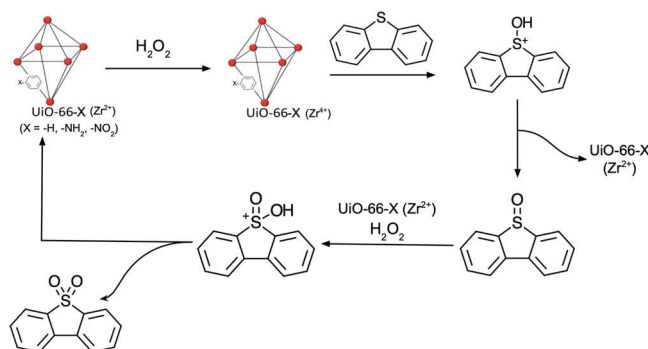
Figure 4. Average percent conversion of DBTO_2 formed over 2 h of oxidative desulfurization.

reached a 96.93% DBTO_2 conversion at 2 h, UiO-66-NH_2 reached a 79.53% conversion at 1.5 h, and UiO-66-NO_2 reached 100.00% conversion at 1 h. Lastly, an ODS reaction was performed without any MOF, showing a 34.89% maximum DBTO_2 conversion at 2 h. All four ODS reactions showed their quickest catalytic conversion from DBT to DBTO_2 within 0.5 h and then slowly plateaued afterward. For the student-run reactions, UiO-66-NO_2 appears to be the most efficient catalyst.

The catalytic performance of the three MOFs aligns with existing literature findings, as the students found. UiO-66-NO_2 exhibits superior activity, followed by UiO-66 , while UiO-66-NH_2 demonstrates the lowest conversion rates. The highest catalytic activity of UiO-66-NO_2 is likely due to its nitro group functionalized linker, which adds electron-withdrawing char-

acter. This aids in making the H_2O_2 complex in the reaction more electrophilic. The mechanisms for ODS (Scheme 1)

Scheme 1. Oxidative Desulfurization of Dibenzothiophene Reaction Scheme Using UiO-66-X ($\text{X} = -\text{H}, -\text{NH}_2, -\text{NO}_2$)



show that the formation of Zr^{4+} is a major contributor for ODS, as DBT molecules coordinate to the Lewis-acid metal sites on the MOF. Having more electron-withdrawing character on the linker would provide activation of more Lewis acid sites and enable more coordination with DBT, resulting in more efficient ODS. Students' experimental data showed that the appearance of an electron-donating group greatly hindered catalytic activity, indicating the need for electron-withdrawing character for the ODS.

Assessing the Structural and Chemical Stability of Catalyst

PXRD measurements (Figure 2) were taken of the MOFs after catalytic performance during ODS in order to check the material's structural durability. Post-ODS MOFs show that the crystallinity of the UiO-66 powders retained major peaks, but some peaks disappeared or shifted, suggesting introduction of defects into the MOFs (Figure 2). Furthermore, FT-IR measurements (Figure 3) were taken of the MOFs after ODS to confirm that the functional groups were still present. Post-ODS results from students show that the organic linker found within the UiO-66 powders remained unchanged after an initial run, confirming the MOFs' structural durability as a catalyst for ODS.

Since UiO-66-NO_2 demonstrated the highest catalytic activity, the students performed recyclability tests (Figure 5). The catalyst was relatively easy to recycle after the initial reaction via vacuum filtration and washing with acetonitrile.

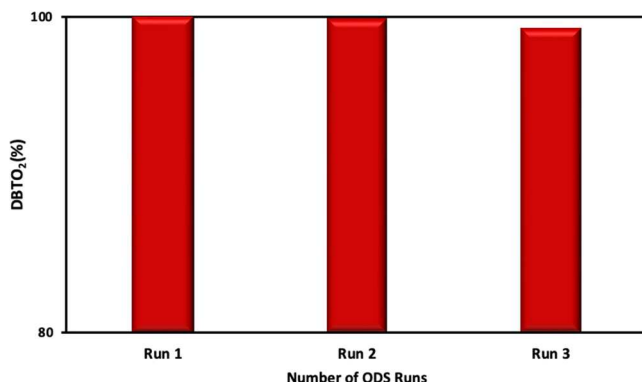


Figure 5. Recyclability of the UiO-66-NO_2 MOF. Each run represents the ODS of DBT, yielding 99.73% conversion of DBT to DBTO_2 .

After a total of three different runs, the catalytic performance of UiO-66-NO_2 maintained a 99.3% conversion rate, suggesting little to no degradation in its performance as shown in Figure 5.

■ STUDENT LEARNING OUTCOMES

To help students understand MOF composition–structure–property relationships, the instructor presented information on:

- Importance of fuel desulfurization
- Composition, morphology, and structures of zirconium-based MOFs
- Spectroscopic analysis
- GC-MS kinetics investigations
- Data analysis and interpretation

Students were then assessed through individually written reports in a scientific journal format and oral presentations in the areas listed above. To probe breadth, the instructor checked that students correctly answered at least 80% of the list of Results and Discussion questions on page S7 of the *Student Handout* in their final report. To probe depth, the instructor checked that students correctly answered all questions from the classroom audience during their oral talks. Students earning a score of 80% or more were classified as achieving learning goals. Students also completed pre- and postsurveys to evaluate their own confidence in laboratory techniques and tasks (Figure S1). After the laboratory activity, all students increased in confidence in their self-assessments of the techniques and tasks.

■ CONCLUSIONS AND FUTURE WORK

The synthesis, characterization, and evaluation of MOFs for the oxidation of DBT to DBTO_2 introduce fundamental chemistry to chemistry and biochemistry majors in the context of using MOFs for fuel desulfurization. Students had the opportunity to synthesize three unique MOFs with different linkers to explore effects of the electronic environment on catalytic conversion of DBT, a toxic fuel additive, to its oxidized and more environmentally friendly form. This lab demonstrates how interconnecting general, organic, inorganic, and materials chemistry in one laboratory project enables students to deepen their thinking through both oral talks and written reports.

■ ASSOCIATED CONTENT

SI Supporting Information

The Supporting Information is available at <https://pubs.acs.org/doi/10.1021/acs.jchemed.4c00297>.

Notes for instructors ([PDF](#))

Lab handout for students ([PDF](#))

Adsorption capacity workup template ([XLSX](#))

■ AUTHOR INFORMATION

Corresponding Author

Monica C. So – California State University, Chico, Chico, California 95929-0210, United States;  orcid.org/0000-0002-9044-4806; Email: mso@csuchico.edu

Authors

Ernesto Lucatero – California State University, Chico, Chico, California 95929-0210, United States

Robabeh Bashiri – California State University, Chico, Chico, California 95929-0210, United States

Complete contact information is available at:
<https://pubs.acs.org/10.1021/acs.jchemed.4c00297>

Notes

The authors declare no competing financial interest.

■ ACKNOWLEDGMENTS

E.L. acknowledges the CSU Chico Student Award for Research and Creativity for funding. M.C.S. and R.B. thank the National Science Foundation (DMR-2137915) for funding. M.C.S. served as Principal Investigator on ACS PRF #65509-UR10 that provided support for E.L. and acknowledges support from Camille and Henry Dreyfus Foundation (TH-23-035) and U.S. Department of Energy, Office of Science, Offices of Basic Energy Sciences and Electricity under contract DE-SC0024581. We would like to finally thank Dr. Lisa Ott at CSU Chico for GC-MS assistance and method development.

■ REFERENCES

- (1) Yoon, S.; Calvo, J. J.; So, M. C. Removal of Acid Orange 7 from Aqueous Solution by Metal-Organic Frameworks. *Crystals* **2019**, *9* (1), 17.
- (2) Adegoke, K. A.; Maxakato, N. W. Porous Metal-Organic Framework (MOF)-Based and MOF-Derived Electrocatalytic Materials for Energy Conversion. *Mater. Today Energy* **2021**, *21*, 100816.
- (3) Cash, A. R.; Penick, J. R.; Todd, C. F.; So, M. C. Escaping the Environmental Crises: Online Escape Rooms for Evaluating Student Data Analysis Skills. *J. Chem. Educ.* **2023**, *100* (11), 4530–4535.
- (4) Yoon, S.; Talin, A. A.; Stavila, V.; Mroz, A. M.; Bennett, T. D.; He, Y.; Keen, D. A.; Hendon, C. H.; Allendorf, M. D.; So, M. C. From N- to p-Type Material: Effect of Metal Ion on Charge Transport in Metal-Organic Materials. *ACS Appl. Mater. Interfaces* **2021**, *13* (44), 52055–52062.
- (5) Barea, E.; Montoro, C.; Navarro, J. A. R. Toxic Gas Removal - Metal-Organic Frameworks for the Capture and Degradation of Toxic Gases and Vapours. *Chem. Soc. Rev.* **2014**, *43* (16), 5419–5430.
- (6) Mason, J. A.; Veenstra, M.; Long, J. R. Evaluating Metal-Organic Frameworks for Natural Gas Storage. *Chem. Sci.* **2014**, *5* (1), 32–51.
- (7) Zhang, Y.; Li, G.; Kong, L.; Lu, H. Deep Oxidative Desulfurization Catalyzed by Ti-Based Metal-Organic Frameworks. *Fuel* **2018**, *219*, 103–110.
- (8) Veisi, H.; Abrifam, M.; Kamangar, S. A.; Pirhayati, M.; Saremi, S. G.; Noroozi, M.; Tamoradi, T.; Karmakar, B. Pd Immobilization Biguanidine Modified Zr-UiO-66 MOF as a Reusable Heterogeneous Catalyst in Suzuki-Miyaura Coupling. *Sci. Rep.* **2021**, *11* (1), 21883.
- (9) Pascanu, V.; González Miera, G.; Inge, A. K.; Martín-Matute, B. Metal-Organic Frameworks as Catalysts for Organic Synthesis: A Critical Perspective. *J. Am. Chem. Soc.* **2019**, *141* (18), 7223–7234.
- (10) Alhumaimess, M. S. Metal-Organic Frameworks and Their Catalytic Applications. *J. Saudi Chem. Soc.* **2020**, *24* (6), 461–473.
- (11) Liao, X.; Wang, X.; Wang, F.; Yao, Y.; Lu, S. Ligand Modified Metal Organic Framework UiO-66 : A Highly Efficient and Stable Catalyst for Oxidative Desulfurization. *J. Inorg. Organomet. Polym. Mater.* **2021**, *31* (2), 756–762.
- (12) Timofeeva, M. N.; Panchenko, V. N.; Jun, J. W.; Hasan, Z.; Matrosova, M. M.; Jhung, S. H. Effects of Linker Substitution on Catalytic Properties of Porous Zirconium Terephthalate UiO-66 in Acetalization of Benzaldehyde with Methanol. *Appl. Catal. Gen.* **2014**, *471*, 91–97.
- (13) Nguyen, H. G. T.; Schweitzer, N. M.; Chang, C.-Y.; Drake, T. L.; So, M. C.; Stair, P. C.; Farha, O. K.; Hupp, J. T.; Nguyen, S. T. Vanadium-Node-Functionalized UiO-66 : A Thermally Stable MOF-Supported Catalyst for the Gas-Phase Oxidative Dehydrogenation of Cyclohexene. *ACS Catal.* **2014**, *4* (8), 2496–2500.

(14) Beyzavi, M. H.; Vermeulen, N. A.; Zhang, K.; So, M.; Kung, C.; Hupp, J. T.; Farha, O. K. Liquid-Phase Epitaxially Grown Metal-Organic Framework Thin Films for Efficient Tandem Catalysis Through Site-Isolation of Catalytic Centers. *ChemPlusChem*. 2016, 81 (8), 708–713.

(15) Vermoortele, F.; Ameloot, R.; Alaerts, L.; Matthessen, R.; Carlier, B.; Fernandez, E. V. R.; Gascon, J.; Kapteijn, F.; De Vos, D. E. Tuning the Catalytic Performance of Metal-Organic Frameworks in Fine Chemistry by Active Site Engineering. *J. Mater. Chem.* 2012, 22 (20), 10313.

(16) Wei, Y.-S.; Zhang, M.; Zou, R.; Xu, Q. Metal-Organic Framework-Based Catalysts with Single Metal Sites. *Chem. Rev.* 2020, 120 (21), 12089–12174.

(17) Roach, B. D.; Forgan, R. S.; Kamenetzky, E.; Parsons, S.; Plieger, P. G.; White, F. J.; Woodhouse, S.; Tasker, P. A. From Gas Phase Observations to Solid State Reality: The Identification and Isolation of Trinuclear Salicylaldoximato Copper Complexes. *Molecules* 2022, 27 (19), 6421.

(18) Todd, C.; Ceballos, C. M.; So, M. C. Synthesis, Characterization, and Evaluation of Metal-Organic Frameworks for Water Decontamination: An Integrated Experiment. *J. Chem. Educ.* 2022, 99 (6), 2392–2398.

(19) Bhadra, B. N.; Jhung, S. H. Oxidative Desulfurization and Denitrogenation of Fuels Using Metal-Organic Framework-Based/-Derived Catalysts. *Appl. Catal. B Environ.* 2019, 259, 118021.

(20) Piscopo, C. G.; Granadeiro, C. M.; Balula, S. S.; Bošković, D. Metal-Organic Framework-Based Catalysts for Oxidative Desulfurization. *ChemCatChem*. 2020, 12 (19), 4721–4731.

(21) Yang, E.-C.; Liu, Z.-Y.; Wu, X.-Y.; Chang, H.; Wang, E.-C.; Zhao, X.-J. CuII, MnII and CuII-Directed Coordination Polymers with Mixed Tetrazolate-Dicarboxylate Heterobridges Exhibiting Spin-Canted, Spin-Frustrated Antiferromagnetism and a Slight Spin-Flop Transition. *Dalton Trans.* 2011, 40 (39), 10082.

(22) Viana, A. M.; Julião, D.; Mirante, F.; Faria, R. G.; De Castro, B.; Balula, S. S.; Cunha-Silva, L. Straightforward Activation of Metal-Organic Framework UiO-66 for Oxidative Desulfurization Processes. *Catal. Today* 2021, 362, 28–34.

(23) Masoomi, M. Y.; Bagheri, M.; Morsali, A. Application of Two Cobalt-Based Metal-Organic Frameworks as Oxidative Desulfurization Catalysts. *Inorg. Chem.* 2015, 54 (23), 11269–11275.

(24) Fu, G.; Bueken, B.; De Vos, D. Zr-Metal-Organic Framework Catalysts for Oxidative Desulfurization and Their Improvement by Postsynthetic Ligand Exchange. *Small Methods* 2018, 2 (12), 1800203.

(25) Janssens, N.; Wee, L. H.; Martens, J. A. Esterification Reaction Utilizing Sense of Smell and Eyesight for Conversion and Catalyst Recovery Monitoring. *J. Chem. Educ.* 2014, 91 (6), 876–879.

(26) Huo, H.-Y.; Liu, Y.-W.; Yuan, M.; Lu, Y.; Wang, J.; Zhu, G.-S.; Liu, S.-X. Synthesis and Characterization of H5PV2Mo10O40@Cu3(BTC)2 and Its Use as a Heterogeneous Catalyst for Oxidative Desulfurization: A Comprehensive Chemistry Laboratory Experiment. *J. Chem. Educ.* 2021, 98 (11), 3580–3586.

(27) Tang, X.; Luo, Y.; Zhang, Z.; Ding, W.; Liu, D.; Wang, J.; Guo, L.; Wen, M. Effects of Functional Groups of -NH₂ and -NO₂ on Water Adsorption Ability of Zr-Based MOFs (UiO-66). *Chem. Phys.* 2021, 543, 111093.

(28) Dinh, H. T.; Tran, N. T.; Trinh, D. X. Investigation into the Adsorption of Methylene Blue and Methyl Orange by UiO-66-NO₂ Nanoparticles. *J. Anal. Methods Chem.* 2021, 2021, 1–10.